SPATIOTEMPORAL DYNAMICS AND CLIMATIC FACTORS AFFECTING NET PRIMARY PRODUCTIVITY IN NIGER RIVER BASIN, FROM 2000 TO 2020

OGBUE, C.[1,2] – IGBOELI, E.[1,2] – YAHAYA, I.[1,2] – YENEAYEHU, F.[1,2] – FU, S. L.[1,2] – CHEN, Y. S.[1,2] – YOU, Y.[1] – WANG, Y. D.[1*]

[1]*National Engineering Technology Research Center for Desert and Oasis Ecological Construction, Xinjiang Institute of Ecology and Geography, Chinese Academy of Sciences, 818 South Beijing Road Urumqi, 830011 Xinjiang, China*

[2]*University of Chinese Academy of Sciences, Beijing 100049, China*

[*]*Corresponding author*
e-mail: wangyd@ms.xjb.ac.cn

(Received 21st Aug 2023; accepted 23rd Oct 2023)

Abstract. Net primary productivity is an essential measure of plant biology and the net flow of carbon between the atmosphere and the terrestrial environment. This aids in comprehending how much carbon is fixed by terrestrial plants and the factors that affect it, thus requiring a thorough grasp of net primary productivity dynamics and how they interact with the climate in arid and humid regions. This study applied remote sensing techniques to evaluate the spatial distribution and climatic variables of the net primary productivity in the Niger River Basin, using the Carnegie Ames Stanford Approach model and correlation analysis. The study revealed that the net primary productivity fell from 338.18 gC/m^2 in 2000 to 334.44 gC/m^2 in 2020. The correlation result shows that while precipitation (R^2=0.87) and actual evapotranspiration (R^2=0.83) revealed a positive correlation, temperature (R^2=0.328), solar radiation (R^2=0.585), and potential evapotranspiration (R^2=0.78) shows a negative correlation with the net primary productivity. The study shows that precipitation has a major influence on changes in the net primary production of the NRB. The results of the study may help to better understand how climate studies affect environmental ecology while recommending policymakers to safeguard the Niger River Basin from activities that can deteriorate the environment.

Keywords: *remote sensing, CASA model, vegetation production, climate variables, precipitation*

Introduction

The development of an ecological civilization will be advantageous both to the present and future generations, considering the fact that ecological construction is an excellent plan for a nation's long-term growth (Xiang-Chao, 2018). The productivity of ecosystems, including vegetation respiration, photosynthesis, and the decomposition pace of organic carbon contents of the soil has been significantly impacted by global climate change (Zhao and Running, 2010; Sun et al., 2022). Amongst the techniques for examining terrestrial vegetation is Net Primary Productivity (NPP) (Jiao et al., 2018; Li et al., 2019). This is fundamental for understanding carbon cycles, managing ecosystems, increasing pasture production (Zhang et al., 2016), agricultural yield (Wang et al., 2019), and climate change (Zhang et al., 2018). NPP measures the amount of organic carbon that was fixed by photosynthesis after taking the respiration of the plant into account (Turner et al., 2006). Despite the fact that anthropogenic activities and a variety of climatic factors influence changes in NPP (Yin et al., 2020), the latter is one of the main causes of fluctuations in NPP (Fu et al., 2023). Climate variables alter the physiological functions of vegetation, which in turn affects NPP (Xuan and Rao, 2023). According to the

http://www.aloki.hu ● ISSN 1589 1623 (Print) ● ISSN1785 0037 (Online)
DOI: http://dx.doi.org/10.15666/aeer/2106_60036022

Intergovernmental Panel on Climate Change's (IPCC) 2021 Sixth Assessment Report, average worldwide land and ocean temperatures increased by about 1.09^{0}C between 2011 and 2020 in comparison to the years 1850 to 1900. Meanwhile, dry and semi-arid regions are where the temperature increase is most noticeable (Zhou et al., 2022).

The Niger River basin (NRB) is a sacrosanct habitat for the nine-member countries because ecosystems, life, and socioeconomic development are largely dependent on the Niger River's water. However, the effects of climate change in the area are widespread and have disadvantaged people and communities who live within precarious environmental systems, unstable systems of governance, and restrained access to water (Goulden and Few, 2011). Some communities such as in Mali, Nigeria, and Niger as well as those in other member countries are affected by this trend (Goulden and Few, 2011). Further evidence from the literature opines that consequences of climate volatility on African ecological systems are already having a detrimental impact on agricultural yield, and future effects are expected to be catastrophic (Niang et al., 2014). Therefore, it is essential to assess ecosystem NPP for sustainable ecological management and land use (Li et al., 2020). With respect to the size of the study area and the intensity of labour associated with direct measurement of NPP, previous studies employed different cost-effective NPP models for estimating vegetation NPP on regional and global scales, using remote sensing techniques. The evaluation of China's terrestrial NPP following urbanization was carried out using the Carnegie Ames Stanford Approach (CASA) (Deyong et al., 2009; Pei et al., 2013). In other studies also (Li et al., 2021; Ren et al., 2021) in China and similarly (Fu et al., 2023) in the Conventional Lake Chad Basin (CLCB), etc. We can elucidate from previous studies, the robustness of the CASA model in estimating NPP and comprehending vegetation dynamics in biomes. Therefore, the study identified research gaps; (1), in-depth studies involving the estimation of NPP have not been conducted in the NRB, considering that a great deal of studies focused on well- or somewhat well-advanced cities with limited spatial scope. (2), the lack of thorough inquiry into specific effects of climate variables on studies of vegetation, and its restoration in the NRB. This study investigated the NPP dynamics of NRB and correlated the climatic variables to determine the influence of significant climatic elements on the rising or falling CASA model-estimated NPP of the study area from 2000 to 2020. Considering the limitation of field data, which causes significant discrepancies in the computational results, and the strain and stress associated with the data assemblage for larger study areas, the study necessitated the application of mathematical models aligned using existing data, as well as remote sensing (Lin, 2009), to investigate the spatial and temporal variations of the NPP in the NRB. To achieve this study, the following research questions were raised; (1), what are the spatiotemporal distribution and trends of NPP in the study area? (2), what are the driving climatic variables of NPP in the NRB? (3), which of the examined climate conditions has the greatest influence on the NPP of NRB? The study used multi-source remote sensing data from 2000 to 2020 that were substituted in the CASA model in an effort to address the aforementioned research questions. The spatiotemporal changes and trends were also examined using the Mann-Kendall trend analysis while the Pearson correlation coefficient analysis was used to determine the relative relationship of the climatic variables with the NPP of the NRB.

http://www.aloki.hu ● ISSN 1589 1623 (Print) ● ISSN1785 0037 (Online)
DOI: http://dx.doi.org/10.15666/aeer/2106_60036022

Materials and Methods

The Study Area

Niger River basin is situated between latitudes 5° and 23° N and longitudes 12° and 17° E, containing the Niger River (length of 4200 km), which is the ninth-longest river in the world and the third-longest in Africa. It rises in the Guinean mountains and falls into the sea via the delta in southern Nigeria and River Benue (1200 km) is its one of its major tributaries. According to the Niger Basin Authority (2014), the NRB is the largest river basin in western Africa covering an area of 2.13 million km^2 (*Fig. 1*), forming a habitat to over 130 million people and spanning throughout nine countries: Benin, Burkina Faso, Cameroon, Chad, Ivory Coast, Guinea, Mali, Niger, and Nigeria (Nexus profile, 2018).

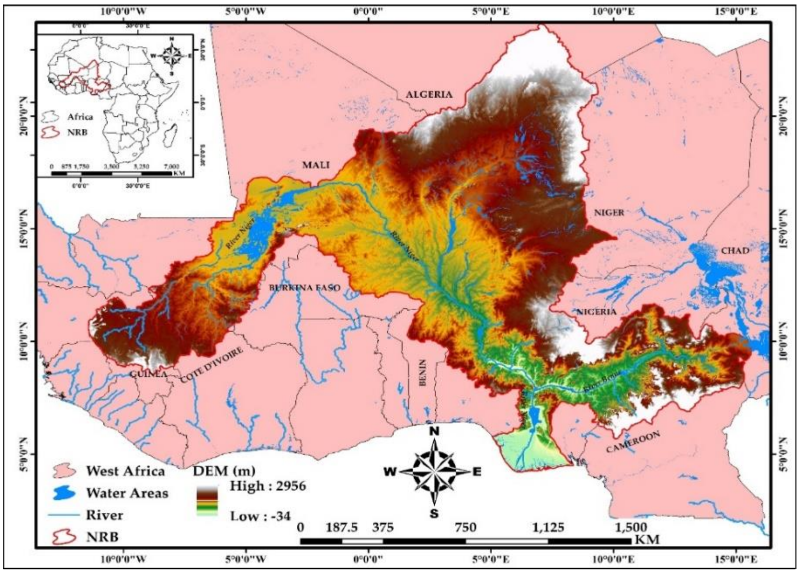

Figure 1. *Niger River Basin (NRB)*

A vulnerable environment characterized by political instability, insecurity, and challenging climatic circumstances is faced by the majority of the member nations, which experience significant urbanization and population expansion (an estimated annual average of 3.2%) (Nexus profile, 2018). The Niger River and its tributaries supply the nine riparian nations with water for drinking, agriculture, industry, energy, and transportation (European Commission, 2016). The annual rainfall ranges from more than 4,000 mm in southern Nigeria and Cameroon to less than 400 mm (and often none at all) on the Sahara Desert's borders in northern Mali and Niger. Climatic zones range from hyper-arid to sub-equatorial semi-arid zones (Aich et al., 2016). Most people in sub-Saharan Africa live in rural areas (61.4%), and most Africans work in the agriculture sector (57.3%), given that agriculture is the largest sector in most sub-Saharan African economies in terms of employment (Dercon and Gollin, 2014). The sector employs about 80% of its workforce, although the agricultural activities in the region have been threatened by rural banditry and regional insecurity (Abdullahi, 2019). Grains, such as maize and rice, as well as root crops, such as yams and cassava, are the most prevalent types of crops. Other major crops include sorghum, millet, rice, peanut, soybean, and beans (Akumaga and Tarhule, 2018).

http://www.aloki.hu ● ISSN 1589 1623 (Print) ● ISSN1785 0037 (Online)
DOI: http://dx.doi.org/10.15666/aeer/2106_60036022

Dataset Acquisition

The Google Earth Engine (GEE) is revolutionary cloud-based platform for the analytical processing of geographically pertinent data. It features a big remote sensing data repository and exceptionally well computing capabilities, which are extremely helpful for processing and extracting massive data through a web-based, programming interface (Wang et al., 2019). The GEE was instrumental in filtering, preprocessing, clipping etc., of the following data:

1. Shuttle Radar Topography Mission (SRTM) based Digital Elevation Model (DEM) data of the study area available from the United States Geological Survey (USGS). The Normalized Difference Vegetation Index (NDVI), obtained from MODIS/061/MOD13A1. The formula as adopted from (Gessesse and Melesse, 2019) is given in *Equation 1*, below.

$$\text{NDVI} = \frac{\text{NIR - RED}}{\text{NIR + RED}} \tag{Eq.1}$$

where;
NIR – reflection in the near-infrared spectrum
RED – reflection in the red range of the spectrum.

2. Meteorological Data: These include; monthly and annual precipitation, solar radiation, evapotranspiration (AET), and potential evapotranspiration (PET) which were all obtained from the Terra-Climate dataset, while the surface temperature was obtained from MODIS/061/MOD11A1.
3. The land use cover change (LUCC) data of 2020 were obtained from the European Space Agency's Climate Change Initiative (ESA-CCI) project data and further reclassified into 8 categories for the purpose of this research. These 8 classes include; Cropland, Forest, Grassland, Sparse vegetation, wetland, urban area, bare land and water body. (*Table 1*) shows the reclassification table while the summary of all the datasets is represented in (*Table 2*).

Data Analysis

NPP Ecosystem CASA Model

The CASA Model has been used for estimating NPP on terrestrial ecosystems because it has proven effective at capturing spatial and temporal NPP dynamics (Potter et al., 1993). The CASA model is a light-use efficiency model based on satellite remote sensing (Zhu et al., 2007) in which NPP is estimated by the production of vegetation-absorbed photosynthetic active radiation (APAR) and actual light use efficiency (ε) by which that radiation is converted to plant biomass increment. In order to estimate NPP, the CASA model uses different forms of remote sensing data which include; NDVI, LUCC, and meteorological datasets such as temperature, solar radiation, precipitation, potential, and actual evapotranspiration. The calculation was performed in Python (3.11) supported in Pycharm Community (2022.3.3). The formula from *Equations 2 to 4*, is given below as extracted from Zhu et al. (2007).

$$\text{NPP}(x, t) = \text{APAR}(x, t) \times \varepsilon(x, t) \tag{Eq.2}$$

$$\text{APAR}(x, t) = \text{SOL}(x, t) \times \text{FPAR}(x, t) \times 0.5 \tag{Eq.3}$$

http://www.aloki.hu ● ISSN 1589 1623 (Print) ● ISSN1785 0037 (Online)
DOI: http://dx.doi.org/10.15666/aeer/2106_60036022

$$\mathrm{FPAR}(x,\ t) = \frac{\mathrm{NDVI}(x,\ t) - \mathrm{NDVI}_{i,min}}{\mathrm{NDVI}_{i,max} - \mathrm{NDVI}_{i,min}} \times (\mathrm{FPAR}_{max} - \mathrm{FPAR}_{min}) + \mathrm{FPAR}_{min} \quad \text{(Eq.4)}$$

where;
NPP = Net primary productivity
APAR = Absorption of photosynthetically active radiation
FPAR = Fraction of photosynthetically active radiation
SOL = Solar radiation
NDVI = Normalized difference vegetation index
ε = Light use efficiency
(x, t) = pixel x in month t.

Table 1. *Land use cover change (LUCC) reclassification adopted from the ESA-CCI land cover dataset*

LUCC	ESA CCI-LC Value	Label
Crop	10,11,12 20 30	Cropland, rainfed, Cropland, irrigated or post-flooding, Mosaic cropland (>50%) / natural vegetation (tree, shrub, herbaceous cover) (<50%)
Forest	40 50 60,61,62 100 110	Mosaic natural vegetation (tree, shrub, herbaceous cover) (>50%) / cropland (<50%) Tree cover, broadleaved, evergreen, closed to open (>15%), Tree cover, broadleaved, deciduous, closed to open (>15%), Mosaic tree and shrub (>50%) / herbaceous cover (<50%), Mosaic herbaceous cover (>50%) / tree and shrub (<50%)
Grassland	120,122,130	Shrubland, Grassland
Sparse Vegetation	150,152,153	Sparse vegetation (tree, shrub, herbaceous cover) (<15%)
Wetlands	170 180	Tree cover, flooded, saline water, Shrub or herbaceous cover, flooded, fresh/saline/brackish water
Artificial area	190	Urban area
Bare land	200,201,202	Bare area
Water	210	Waterbody

Table 2. *Data sources and basic characteristics*

Dataset Category	Dataset Source	Data Processing Interface	Study Year	Spatial resolution(meters)
Solar Radiation	TerraClimate	GEE	2000 – 2020	4638.3
Potential evapotranspiration	TerraClimate	GEE	2000 – 2020	4638.3
evapotranspiration	TerraClimate	GEE	2000 – 2020	4638.3
Precipitation	TerraClimate	GEE	2000 – 2020	4638.3
NDVI	MODIS/061/MOD13A1	GEE	2000 – 2020	500
Surface temperature	MODIS/061/MOD11A1.	GEE	2000 – 2020	1000
Land Cover	ESA CCI	ARCMAP 10.8	2000 – 2020	300

NPP (x, t) is the NPP (gC/m^2) of pixel x in month t; ε(x, t) represents the actual value of the light energy utilization rate of pixel x in month t, which can be obtained by estimating the impact of surface temperature and water stress on the maximum light

http://www.aloki.hu ● ISSN 1589 1623 (Print) ● ISSN1785 0037 (Online)
DOI: http://dx.doi.org/10.15666/aeer/2106_60036022

energy use efficiency under ideal conditions. APAR(x, t) is the absorption of photosynthetically active radiation (MJ m^{-2}) of pixel x in month t; SOL(x, t) is the total solar radiation of pixel x in month t (unit: MJ m^{-2}); FPAR(x, t) is the absorption ratio of photosynthetically active radiation (no unit); 0.5 is the ratio of the effective solar radiation used by vegetation to total solar radiation, which is a constant. For different vegetation types, FPAR is estimated by the maximum and minimum values of NDVI of the vegetation type and the corresponding maximum and minimum values of FPAR. The improved results of the previous studies determine the values of $NDVI_{max}$, $NDVI_{min}$ and light energy use efficiency ε for different land cover types (Zheng et al., 2020). The formula is stated in *Equation 5*, below.

$$\varepsilon_{(x,t)} = T_{\tau 1(x,t)} \times T_{\tau 2(x,t)} \times W_{\tau(x,t)} \times \varepsilon_{max} \qquad \text{(Eq.5)}$$

where;
ε = Light use efficiency
$T_{\tau 1}$ = Low-temperature effect
$T_{\tau 2}$ = High-temperature effect
W_{τ} = soil moisture stress
(x, t) = pixel x in month t.

$T_{\tau 1}$, $T_{\tau 2}$, w_{τ}, and ε_{max} indicate the effects of low and high temperature, soil moisture, and the maximum light used applied on LUE respectively. Detailed calculation steps are also available in some previous relevant studies (Zhu et al., 2007).

Mann–Kendall Trend and Theil-Sen's Slope Analysis

In this work, the trend analysis of NPP was determined using the Mann-Kendall trend significance test and Theil-Sen's slope. Long time series studies of vegetation on the pixel scale commonly use Theil-Sen's slope, which doesn't require the data to follow a specific distribution model or get influenced by outliers (Liu et al., 2021; Rong and Long, 2021; Li et al., 2022). This method quantifies the changing trend slope and the formula is given in *Equation 6*, as follows:

$$\beta = median\left(\frac{NPPj - NPPi}{j - i}\right) 2000 \leq i < j \leq 2020 \qquad \text{(Eq.6)}$$

where;
β = Calculated slope
NPP = Net Primary Productivity
i, j = Changes in time series.

1 < j < i < n, when $\beta > 0$, the changing trend of the time series data increases; when $\beta < 0$, the changing trend of the time series data is reduced. Because β is a non-normalized quantity, it is impossible to determine the importance of a trend shift on its own. Therefore, to achieve the significance test of the trend, it is combined with the Mann–Kendall method. Mann–Kendall is a non-parametric statistical test used to judge the significance of trends. This method is used to evaluate the significance of the NPP trend. The formula is represented in *Equations 7 to 10* below.

http://www.aloki.hu ● ISSN 1589 1623 (Print) ● ISSN1785 0037 (Online)
DOI: http://dx.doi.org/10.15666/aeer/2106_60036022

$$S = \sum_{i=1}^{n-1} \sum_{j=i+1}^{n} sgn(NPP_j - NPP_i) 2000 \leq i < j \leq 2020 \quad \text{(Eq.7)}$$

$$sgn(NPP_j - NPP_i) = \begin{cases} 1 & if(NPP_j - NPP_i > 0) \\ 0 & if(NPP_j - NPP_i = 0) \\ -1 & if(NPP_j - NPP_i < 0) \end{cases} \quad \text{(Eq.8)}$$

$$Z = \begin{cases} \dfrac{S-1}{\sqrt{var(s)}} & S > 0 \\ 0 & S = 0 \\ \dfrac{S+1}{\sqrt{var(s)}} & S < 0 \end{cases} \quad \text{(Eq.9)}$$

$$Var(S) = \frac{n(n-1)(2n+5) - \sum_{i=1}^{m} t_i(t_i-1)(2t_i+5)}{18} \quad \text{(Eq.10)}$$

where;
S = sum of elements
Var = Variance
t_i = varied number of times
Z = Zscore standardize significant level
n = total number of possible pairs of data.

S is the test statistics sum; sgn is a sign function; n is the length of the time series. This research considered a time series of 21 years; therefore, Z is the standardized statistics used to test the trend at a significant level of $\alpha = 0.05$. A positive β indicates a positive trend, while a negative β is vice versa. If the absolute value of Z is greater than 1.96, it indicates that the trend has passed the significance test level. Thus, the H_0 for this test is that there is no significant trend in the NPP series of the NRB.

Analysis of Correlation

The linear relationship between two continuous variables can be evaluated using the Pearson correlation coefficient R, which measures the strength of association, and varies from −1 to +1 (Cleophas et al., 2018).

Using pixel-based Pearson correlation, the intensity of the primary causal meteorological variables in connection to NPP dynamics in the NRB was calculated. The formula is given in *Equation 11*, as;

$$R = \frac{\sum_{i=1}^{n}(X_i - \bar{X})(Y_i - \bar{Y})}{\sqrt{\sum_{i=1}^{n}(X_i - \bar{X})^2 \sum_{i=1}^{n}(Y_i - \bar{Y})^2}} \quad \text{(Eq.11)}$$

where,
R = Correlation, n= number of variables, $\sum xy$ = sum of product of paired variables, $\sum x$ = sum of the x variable, $\sum y$= sum of the y variable, $\sum x^2$ = sum of the squared x variable, $\sum y^2$ = sum of the squared y variable, $\bar{X}$ = x mean, $\bar{Y}$ = y mean.

http://www.aloki.hu ● ISSN 1589 1623 (Print) ● ISSN1785 0037 (Online)
DOI: http://dx.doi.org/10.15666/aeer/2106_60036022

Results

Spatial Variations of NPP in the NRB

The mean annual NPP for the NRB through the 21 years of investigation was 349.20 gC/m^2 and showed a significant regional variation. The raster NPP output was reclassified into five categories, with corresponding values shown in (*Fig. 2*). The observed NPP of NRB was distributed spatially in a south-to-north direction, with total values ranging from 0 to 1353gC/m^2.

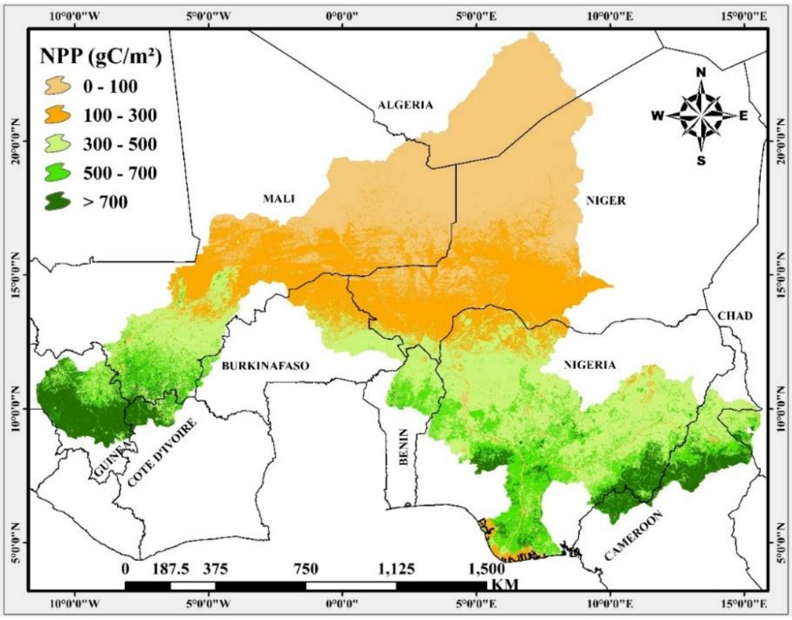

Figure 2. *Spatial distribution of average Net Primary Productivity (NPP) from 2000 to 2020 in the NRB*

While the NPP values declined toward Mali, Niger, the northern part of Nigeria, and a portion of Chad, the areas with noticeably higher NPP are spread across the southern part of Nigeria, north-eastern Benin, north-western Cote d'Ivoire, north-eastern Guinea, and part of Cameroon. The area and percentage of the indicated land cover types of NRB in 2020 are given in (*Fig. 3b*), as distinct types of land degradation are linked to some of the important causes of long-term declines in NPP, while (*Table 3*), below displays the extracted biophysical characteristics for each LUCC type from 2000 to 2020.

Analysis of NPP Variations amongst Individual Biomes

Fig. 3a illustrates the computed NPP values for various biomes in response to changes in LUCC, whereas *Fig. 3c*, depicts a fluctuating simultaneous increase or reduction in NPP values over a 21-year period in each terrestrial ecosystem. The urban area's NPP showed the greatest decline (-211.29 gC/m^2) by 56% (area of 4904.98 km^2), accounting for the largest possible negative NPP change in NRB. The investigation uncovered further areas of negative changes in NPP, such as in forest areas (-13.01 gC/m^2) and bare lands (-9.99 gC/m^2) at 1.96% and 11.37%, respectively. The study also revealed a positive change in wetlands (21.17 gC/m^2), water bodies (0.95 gC/m^2), and sparse vegetation (15.23 gC/m^2) at 8.79%, 0.62%, and 9.13%, respectively, while wetlands and places with

http://www.aloki.hu ● ISSN 1589 1623 (Print) ● ISSN1785 0037 (Online)
DOI: http://dx.doi.org/10.15666/aeer/2106_60036022

sparse vegetation saw the most increase in NPP, with respective areas of 11378.7 km^2 and 1427.54 km^2 as shown in *Fig. 3c*. The LUCC map of the NRB is shown in *Fig. 4*.

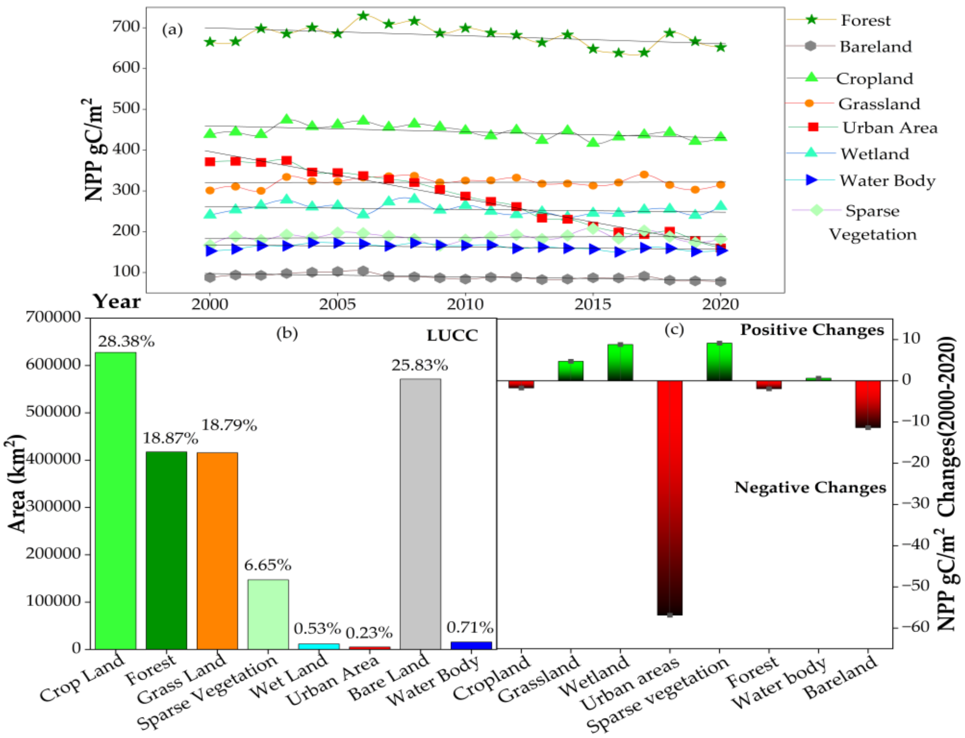

Figure 3. *Statistic information on NPP of the NRB: (a) Inter-annual average NPP in each terrestrial ecosystem from 2000 to 2020; (b) Area (km^2) and percentage of different LUCC in NRB; (c) Observed NPP changes in different terrestrial ecosystems in NRB*

Table 3. *Annual average data statistics of different LUCCs in NRB from 2000 to 2020.*

Biophysical Parameters	**Cropland**	**Grassland**	**Wetland**	**Urban Area**	**Sparse Vegetation**	**Forest**	**Water Body**	**Bareland**
NDVI	0.37	0.28	0.33	0.33	0.15	0.52	0.20	0.11
Solar Radiation (w/m^2)	226.41	238.61	199.21	203.03	250.84	209.62	211.56	257.18
Precipitation (mm)	77.15	53.77	206.06	124.01	25.02	111.14	130.16	11.72
Evapotranspiration (mm)	62.52	44.68	75.74	76.07	22.87	77.32	71.25	10.80
Potential Evapotranspiration (mm)	158.94	179.10	130.01	135.36	204.31	135.70	142.85	218.07
Surface Temperature (^{0}C)	35.85	37.23	28.83	33.96	39.54	32.10	30.01	40.98

Temporal Variation Characteristics of NPP in the NRB

Through the chronicles of the time, the study analyzed changes in the average NPP values recorded in the NRB, and the results showed that the NPP values fell from 338.18(gC/m^2) in 2000 to 334.44(gC/m^2) in 2020. *Fig. 5*, shows the raster output of NPP for 2000 and 2020 as well as the raster rate of change between the two study years.

http://www.aloki.hu ● ISSN 1589 1623 (Print) ● ISSN1785 0037 (Online)
DOI: http://dx.doi.org/10.15666/aeer/2106_60036022

Throughout the study period, the yearly NPP in NRB generally displayed a declining trend. The NPP for the study region first had an upward trend, which peaked between 2006 and 2008, followed by a downward trend towards 2020. *Fig. 6a* shows the NPP values and spatial distribution of between 2000 and 2020. We excluded H_0 and accepted H_1 as mentioned earlier in the Mann-Kendall test at the methodology section since the raster output of the trend analysis in *Fig. 6b*, revealed a statistically significant result, showing areas of negative and positive trends in NPP. The northern parts of Mali and Niger, as well as a larger chunk of north-eastern and western Nigeria, Guinea, and a section of Chad, are the key regions that have undergone a negative change in NPP. While the Sahel lines of Mali, Niger, and Nigeria (the confluence area of the River Niger – Benue trough) were among the sections that showed positive trend changes in NPP. This result coincides with the findings on declining trends in vegetation productivity in the Sahel region of the Chad basin (Ardö et al., 2018; Fu et al., 2023). Nigeria for instance shows a notable decline in NPP, which is in accordance with Abdi et al. (2014).

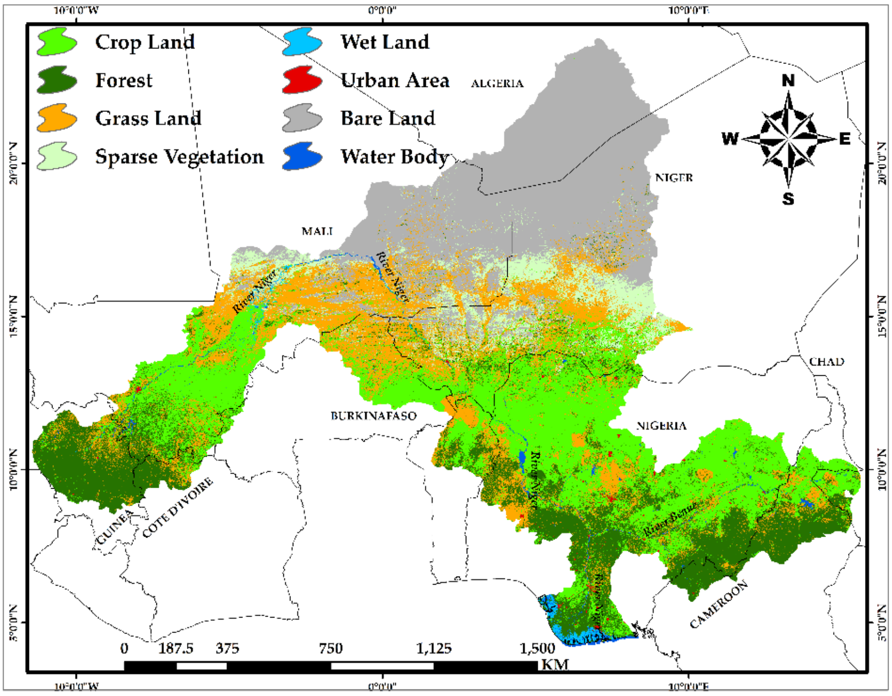

Figure 4. *LUCC Map of the NRB, 2020*

Responses of NPP Spatial Variation to Climatic Factors in NRB

The relationship between climate factors and NPP is a persistent area of scientific study (Wang et al., 2010). For instance, some previous studies (Liu et al., 2019; Yuan et al., 2021; Kayiranga et al., 2022), have correlated precipitation and in some cases with temperature, against primary productivity data of a given area. In the course of the analysis, the study considered the input parameters of the CASA model in conjunction with Thornthwaite Memorial Model for estimating vegetation Production (Lieth and Box, 1972), to determine the degree of relationship each set of climatic factor has on the NPP. Therefore, we performed a pixel-level Pearson correlation analysis at the 95% significance level ($p < 0.05$), between some climatic variables and NPP from 2000 to

http://www.aloki.hu ● ISSN 1589 1623 (Print) ● ISSN1785 0037 (Online)
DOI: http://dx.doi.org/10.15666/aeer/2106_60036022

2020. These climatic variables include: actual evapotranspiration, potential evapotranspiration, total solar radiation, precipitation, and temperature as seen in *Fig. 7*, while *Fig. 8* shows the average spatial distribution of these climatic factors in the NRB.

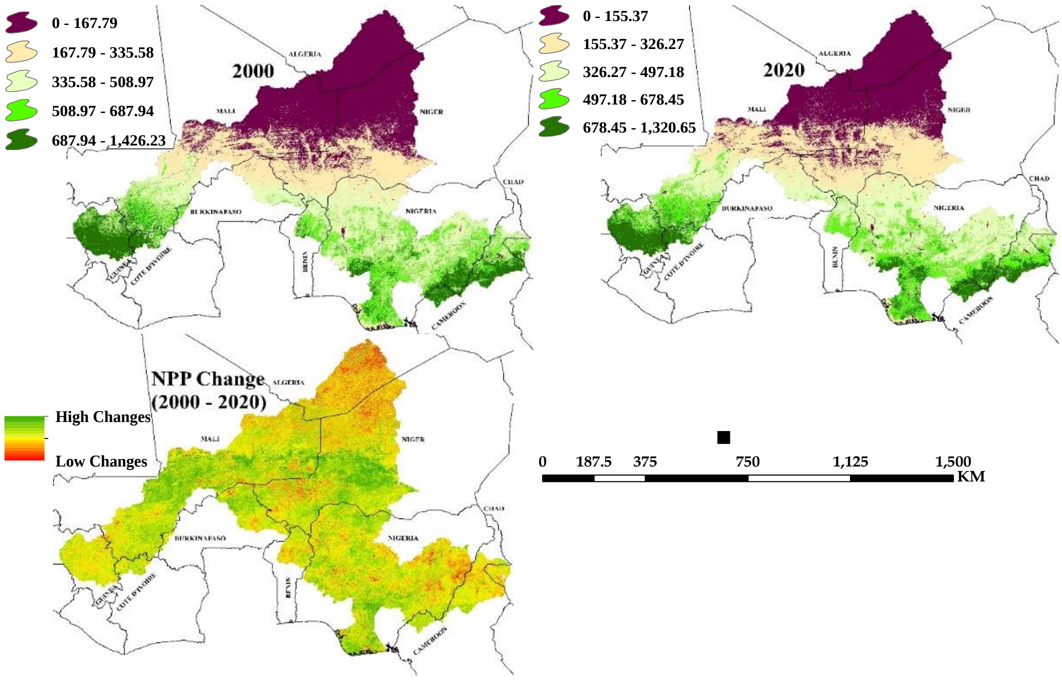

Figure 5. *NPP of 2000 and 2020, and the Rate of Change*

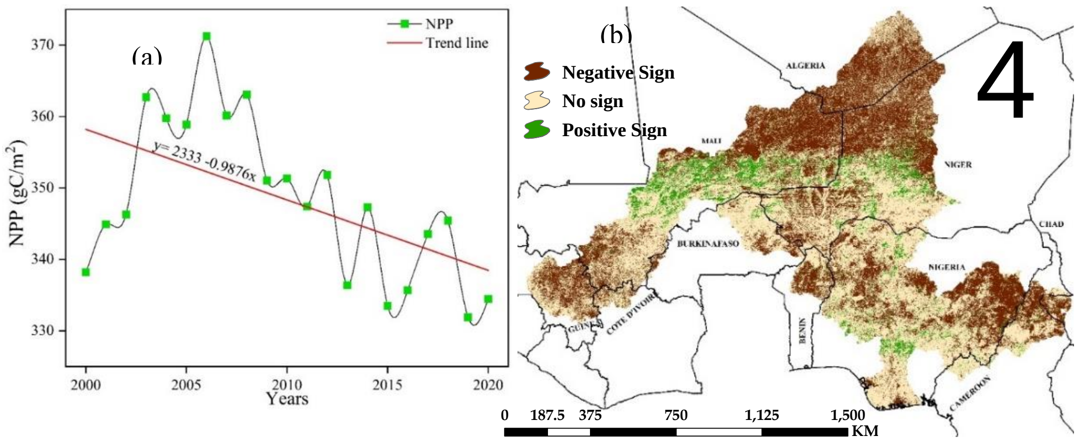

Figure 6. *(a) Annual Average NPP values in NRB from 2000 to 2020; (b) NPP trends in NRB from 2000 to 2020*

While PET, solar radiation, and temperature all displayed a negative association with NPP (r^2 = 0.328, 0.58, and 0.78, respectively), precipitation and AET showed a positive correlation with NPP at coefficients of 0.87 and 0.83, respectively. As seen in *Fig. 9*, NPP with PET demonstrated the strongest negative association, which was then followed by solar radiation and temperature in decreasing order while precipitation with NPP demonstrated the strongest positive correlation, which was then followed by AET.

http://www.aloki.hu ● ISSN 1589 1623 (Print) ● ISSN1785 0037 (Online)
DOI: http://dx.doi.org/10.15666/aeer/2106_60036022

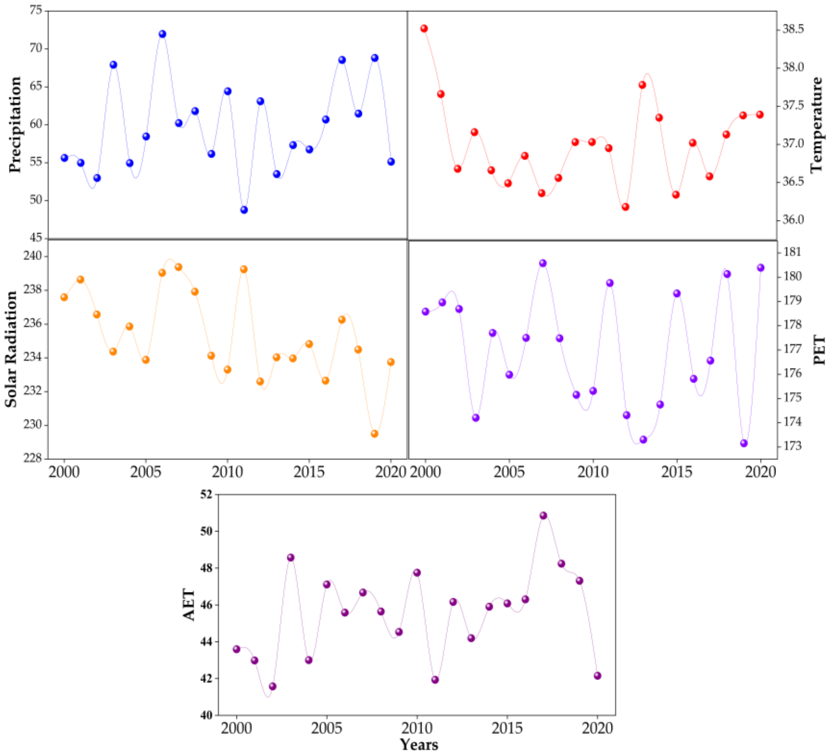

Figure 7. Average yearly data of different climatic variables in the NRB from 2000 to 2020

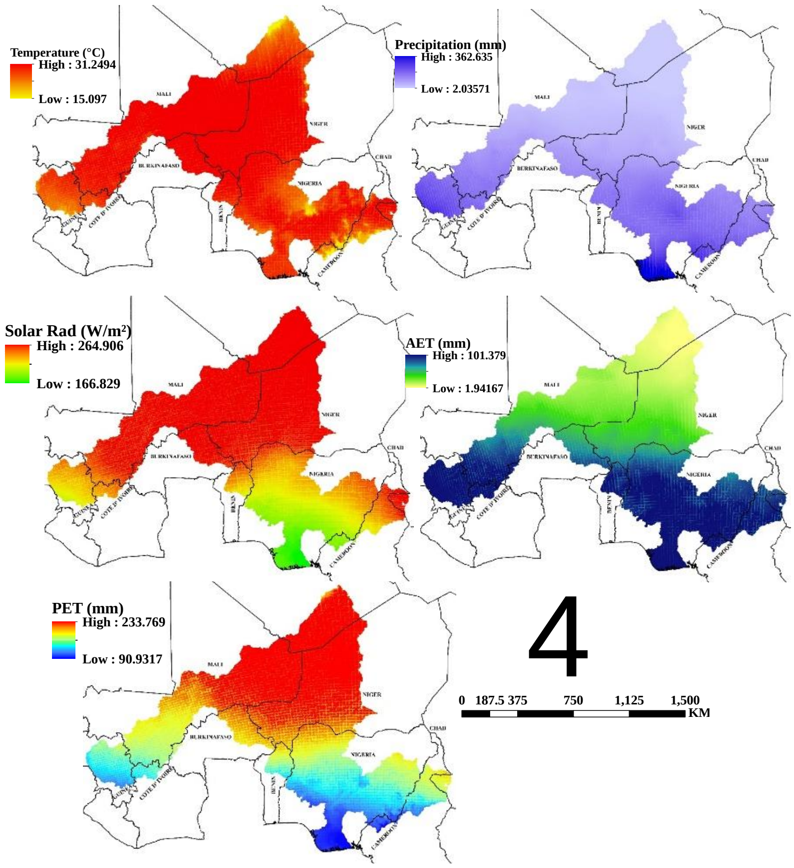

Figure 8. Spatial distribution of the climatic variables in the NRB from 2000 to 2020

http://www.aloki.hu ● ISSN 1589 1623 (Print) ● ISSN1785 0037 (Online)
DOI: http://dx.doi.org/10.15666/aeer/2106_60036022

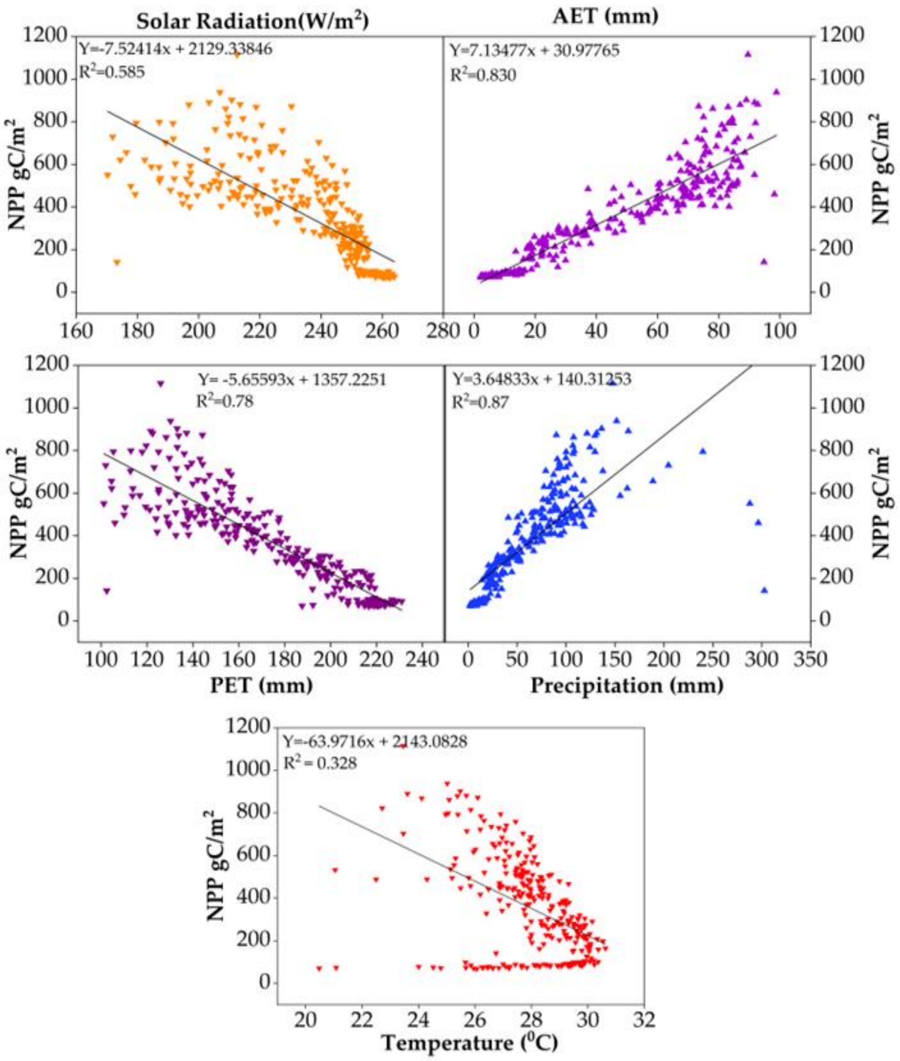

Figure 9. *Correlation Analysis Results of NPP With Climatic Variables in the NRB*

Discussion

Based on substantial numerical evidence provided by this research, which is subject to critics, the study portrayed NPP increment/reduction in the NRB and identified key drivers. More so, the NPP value of 349.20 gC/m^2 in the NRB is in line with other CASA model simulation findings reported in the literature, such as the NPP value of 392.64 gC/m^2 obtained in the Conventional lake Chad region (Fu et al., 2023). This research showed that the NPP of the NRB indicates a falling trend, with the exception of the year 2006, which recorded an increase in NPP as seen in *Fig. 6*. These observed variations in NPP are related to the identified vegetation and land cover categories in the study area. The southern part of the research area, where forest, cropland, and grassland are predominant falls within the Guinea savannah and tropical rainforest vegetation regions of the NRB. There, the soil is rich and ideal for growing a variety of crops (Liu et al., 2021). The northern part of the research area, which is marked by an arid climate, barren soil, and little vegetation, has low NPP values, given that in dry areas, water is the scarcest resource. As a result, water becomes scarce commodity for primary production (Sala et al., 2015).

http://www.aloki.hu ● ISSN 1589 1623 (Print) ● ISSN1785 0037 (Online)
DOI: http://dx.doi.org/10.15666/aeer/2106_60036022

Although sustaining the equilibrium of water on Earth requires both AET and PET processes, PET is predominant as it evaluates the atmosphere's ability to evaporate water from its surface (Dong et al., 2020), when there is no regulation over water. This was demonstrated by the correlation results between PET and AET with NPP, the research area's northern Sahel region is dry and has low levels of NPP, hence the impact of PET was evident there. This suggests the cause of the strong negative correlation between PET and NPP. On the other hand, due to the higher values of NPP and the greater amount of vegetation in the southern part of the research zone, the circulation of water is controlled. The trees usually store more water than they transpire while still facilitating evapotranspiration (Holder, 2004), and increases the atmospheric humidity, which would still convert into precipitation, perceived as rain on the earth's surface. The high positive correlation between precipitation and AET with NPP indicates that rainfall significantly affects the growth of the vegetative layer, and consequently exerts a positive influence on the NPP. Thus, insinuating the main climatic variable influencing the values of NPP in the NRB (*Fig. 9*).

Complex interactions between the land and climate can also be demonstrated in LUCC, which is impacted by both precipitation and solar radiation. Precipitation is one of the main climatic factors affecting plant productivity and we observed from the correlation results that an increase in precipitation significantly increases the values of NPP in the NRB. This is also in accordance with Wang (2022), which evaluated how responsive above- and below-ground net primary productivity was to precipitation, indicating that more precipitation might boost ecosystem productivity. The southern part of the NRB, where the vegetation grows greener shows a stronger relationship between rainfall and NPP. This is due to the NRB's southern section receiving more rainfall and having sufficient amounts of groundwater, which balances the atmosphere by regulating evapotranspiration, carbon presence in the atmosphere, and solar radiation. More plants promote higher precipitation by removing moisture from the soil and redistributing it into the atmosphere, from where it can fall again as rain with the entire circle resulting in more vegetation and in turn, increased NPP. Our study also revealed that solar radiation shows a strong negative correlation ($r^2 = 0.78$) with NPP, revealing a decrease in values of NPP with an increase in solar radiation. *Fig. 8* shows high solar radiation in the northern part of the study area, characterized by arid bare area with low values of NPP.

As we know, the sun powers the planet's climate system, but differences in the nature and amount of solar radiation may lead to alterations in the climate. Plants employ this solar energy to form and break bonds of chemicals, which gives them the vitality they need to grow. However, high radiation rates affected by LUCC could be detrimental to the terrestrial ecosystem. The evapotranspiration of soil water can be impacted by solar radiation in the same way that precipitation can raise humidity levels in both soil and air moisture content, and the soil capacity to retain water is also affected by intense solar radiation thereby leaving the soil with little or no water to support plants' growth. This is evident in the spatial distribution of NPP in the study area (*Fig. 2*), given that NPP is higher in forest areas of the southern part than towards the bare area of the northern part, which recorded high solar radiation.

More so, dynamics in albedo is exacerbated by LUCC especially from densely vegetation areas to barren areas. Low-albedo vegetation facilitates evapotranspiration, the process through which water vaporizes into the atmosphere while the warmed-up bare surface area with high albedo will reflect more solar radiation thereby allowing for the limited possibility of plant survival in the study area, resulting to decreased values of NPP

http://www.aloki.hu ● ISSN 1589 1623 (Print) ● ISSN1785 0037 (Online)
DOI: http://dx.doi.org/10.15666/aeer/2106_60036022

in the region affected. This implies that high levels of solar radiation have an impact on the climate of the study region, which in turn influences the LUCC due to the heat exchange interaction between the ground and the atmosphere. However, this is not the case in the southern portion of the research area, which is home to a humid tropical rainforest with low albedo and higher amounts of precipitation. Other studies also supports the claim that precipitation has a significant impact on vegetation productivity (Zhuang et al., 2010; Piao et al., 2012; Liu et al., 2019; Ren et al., 2021; Zhang et al., 2020), including semi-arid regions of the Lake Chad Basin (Fu et al., 2023). *Fig. 10* shows a distinct relationship between precipitation and the NPP of NRB.

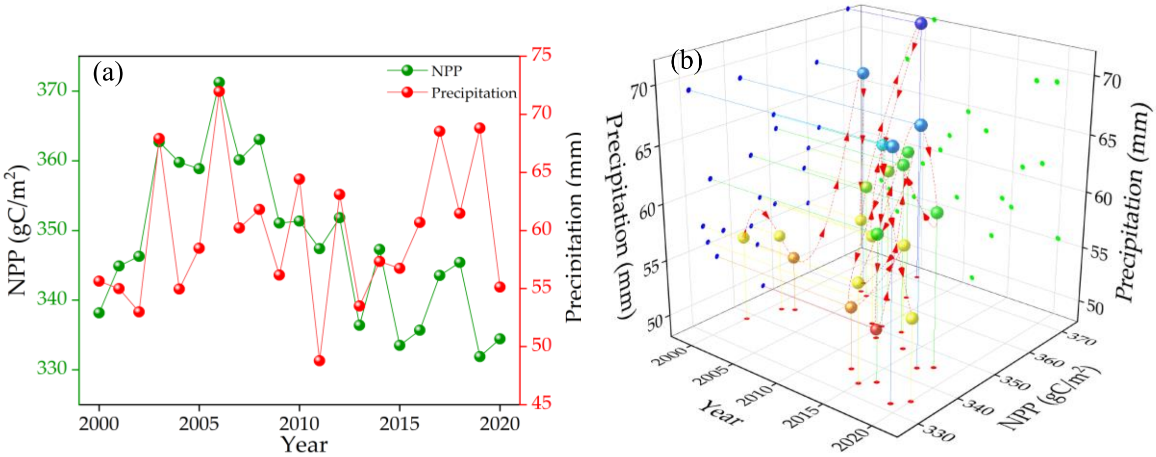

***Figure 10.** Effect of precipitation on NPP of NRB. (a) Linear relation between NPP and precipitation; (b) Distinct NPP value reactions to increasing or decreasing precipitation values*

Therefore, it is crucial to preserve the plant cover in the NRB in order to regulate solar radiation and maintain precipitation levels, which will raise the value of NPP in the study area. This will assist in increasing agricultural productivity and even combat the threat of desertification, thereby preventing a significant adverse impact on food production.

Additionally, the negative NPP trend recorded in the bare land of the study area (420990.5 km^2), further illustrates the aggravating effect of climate change on the NPP of the NRB. The southward expansion of the bare land may lead to a reduction in NPP viz a viz desert encroachment towards the southern portion of the NRB (*Fig. 11*). Although there have been a strategy associated with the ground-breaking African-led Great Green Wall initiative in collaboration with UNCCD. A project designed to rehabilitate the continent's devastated landscapes and improve millions of lives in the Sahel area (UNCCD, 2007).

Our study demonstrates that the NPP of the NRB is unevenly distributed throughout the study area, declining from the southernmost point of Nigeria to the Sahelian borders of Niger and Mali in a south-to-north manner. The study also found that from 2000 and 2020, NPP had a declining trend while amongst the examined climatic driving factors, precipitation was identified as the most influential to NPP changes in the study area.

The study equally shaded some challenges, such as the scale of the researched area resulting in certain limitations, particularly in the areas of data aggregation, sources, and reach, notwithstanding the useful conclusions that this study gave for the betterment of the NRB's future. Likewise, the integration of several software packages used to analyze the studied data could result in undetectable inaccuracies, especially in NPP calculation.

http://www.aloki.hu ● ISSN 1589 1623 (Print) ● ISSN1785 0037 (Online)
DOI: http://dx.doi.org/10.15666/aeer/2106_60036022

As past studies have shown, there are additional uncertainties regarding the satellite remotely sensed data for the CASA model with respect to the optical satellite sensors which also require improvement (Ndayisaba et al., 2016; Kayiranga et al., 2017).

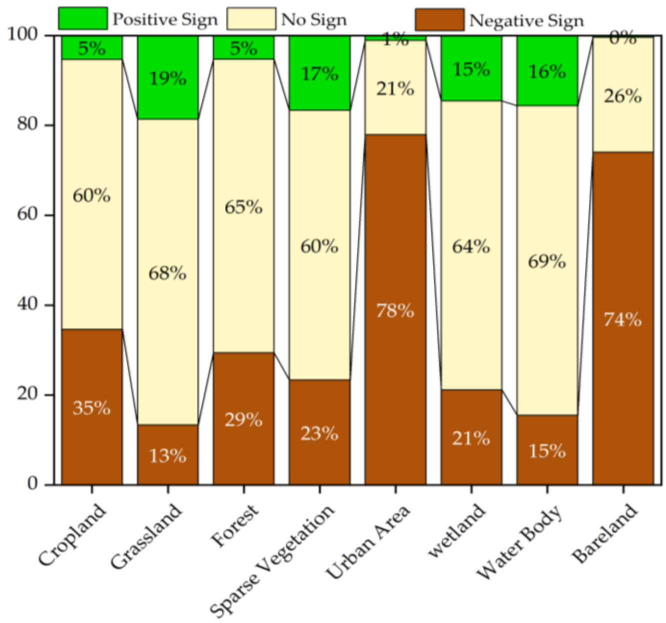

Figure 11. *NPP variation significance in each terrestrial ecosystem*

Conclusion

This research investigated the spatiotemporal dynamics, trends, and factors of NPP variations in the NRB. The study shows that the NPP of the NRB is not uniformly spread throughout the study area, decreasing in a south-to-north direction, from the southern extent of Nigeria to the Sahelian borders of Niger and Mali. The study also revealed that NPP showed a decreasing trend from 2000 to 2020. Amongst the climatic driver variables examined in the study area, precipitation, and AET were positively correlated with NPP, while PET, solar radiation, and temperature were negatively correlated with NPP. Our study elucidated that amongst these climatic variables, precipitation was related as the most influential climatic element of NPP dynamics in the NRB, according to the results of the correlation analyses. It is clear that climate change has a substantial impact on the NPP of NRB. Therefore, research on the relationship between NPP and climatic factors is essential for revealing how well ecosystems can adapt to global warming and environmental management for increased vegetation productivity and building a healthy ecological habitat.

Recommendations

- The Niger River Basin Authority and other policy-makers should thereby ensure that the inhabitants of the NRB conform to a living guide that will strongly refute activities that exacerbates the negative impact of climate change in the NRB.
- The government and other policy makers should promote sustainable environmental policies that protects the use of land in the Niger River Basin and put strong sanctions in place for defaulters.

http://www.aloki.hu ● ISSN 1589 1623 (Print) ● ISSN1785 0037 (Online)
DOI: http://dx.doi.org/10.15666/aeer/2106_60036022

- Additionally, more tree planting should be encouraged in accordance with the Great Green Wall initiative, for the restoration of NPP of NRB, and greening the Sahel region at large.
- The study also recommends more investigation into topics that will identify and analyze more variables that affect NPP changes in the in the Niger River Basin.

Author Contributions. O.C; Conceptualization, Methodology, Investigation, and Writing – original draft, I.E and Y.Y; Data curation and Formal analysis, F.S and C.Y; Software, Y.I and Y.F; Writing – review & editing, W.Y; Funding acquisition and Supervision. All authors contributed critically to the drafts and gave final approval for publication.

Conflicts of Interests. The authors declare no conflict of interests.

Data Availability Statement. The data used in the course of this research are shown in the manuscript and available from the author upon request.

Acknowledgments. The authors wish to thank the Integration and application of appropriate technologies for desertification control in Africa (Grant No. SAJC202108), the Science and Technology Partnership Program and International Science and Technology Cooperation Program of Shanghai Cooperation Organization [Grant No. 2022E01012], and the Alliance of International Science Organizations of Association [Grant No. ANSO-PA-2020-15]. Our thanks also go to the support of the key technical talent project of Chinese Academy of Sciences (Research on desertification technology along the “Belt and Road”), the “Tianchi doctor program” of Xinjiang Uygur Autonomous Region in 2020 and Xinjiang Institute of Ecology and Geography, Urumqi, University of Chinese Academy of Sciences, China.

REFERENCES

[1] Abdi, A. M., Seaquist, J., Tenenbaum, D. E., Eklundh, L., Ardö, J. (2014): The supply and demand of net primary production in the Sahel. – Environmental Research Letters 9(9). https://doi.org/10.1088/1748-9326/9/9/094003.

[2] Abdullahi, A. (2019): Rural Banditry, Regional Security and Integration in West Africa. – Journal of Social and Political Sciences 2(3): 644-654. https://doi.org/10.31014/aior.1991.02.03.107.

[3] Aich, V., Liersch, S., Vetter, T., Fournet, S., Andersson, J. C. M., Calmanti, S., van Weert, F. H. A., Hattermann, F. F., Paton, E. N. (2016): Flood projections within the Niger River Basin under future land use and climate change. – Science of the Total Environment 562: 666-677. https://doi.org/10.1016/j.scitotenv.2016.04.021.

[4] Akumaga, U., Tarhule, A. (2018): Projected changes in intra-season rainfall characteristics in the Niger River Basin, West Africa. – Atmosphere 9(12): 1983-1985. https://doi.org/10.3390/atmos9120497.

[5] Ardö, J., Tagesson, T., Jamali, S., Khatir, A. (2018): MODIS EVI-based net primary production in the Sahel 2000–2014. – International Journal of Applied Earth Observation and Geoinformation 65(October 2017): 35-45. https://doi.org/10.1016/j.jag.2017.10.002.

[6] Cleophas, T. J., Zwinderman, A. H., Cleophas, T. J., Zwinderman, A. H. (2018): Bayesian Pearson correlation analysis. – Modern Bayesian Statistics in Clinical Research, pp. 111-118.

[7] Dercon, S., Gollin, D. (2014): Agriculture in African development: Theories and strategies. – Annual Review of Resource Economics 6(1): 471-492. https://doi.org/10.1146/annurev-resource-100913-012706.

[8] Deyong, Y., Hongbo, S., Peijun, S., Wenquan, Z., Yaozhong, P. (2009): How does the conversion of land cover to urban use affect net primary productivity? A case study in Shenzhen city, China. – Agricultural and Forest Meteorology 149(11): 2054-2060.

https://doi.org/10.1016/j.agrformet.2009.07.012.
[9] Dong, W., Li, C., Hu, Q., Pan, F., Bhandari, J., Sun, Z. (2020): Potential Evapotranspiration Reduction and Its Influence on Crop Yield in the North China Plain in 1961-2014. – Advances in Meteorology, Article ID: 3691421.
[10] European Commision. (2016): Towards a Niger Basin Nexus Dialogues Project. – Exploratory Mission Report.
[11] Fu, S., Zhou, Y., Lei, J., Zhou, N. (2023): Changes in the Spatiotemporal of Net Primary Productivity in the Conventional Lake Chad Basin between 2001 and 2020 Based on CASA Model. – Atmosphere 14(2): 232. https://doi.org/10.3390/atmos14020232.
[12] Gessesse, A. A., Melesse, A. M. (2019): Temporal relationships between time series CHIRPS-rainfall estimation and eMODIS-NDVI satellite images in Amhara Region, Ethiopia. – In Extreme Hydrology and Climate Variability: Monitoring, Modelling, Adaptation and Mitigation. Elsevier Inc. https://doi.org/10.1016/B978-0-12-815998-9.00008-7.
[13] Goulden, M., Few, R. (2011): Climate Change, Water and Conflict in the Niger River Basin. – Usaid, December, pp. 1–70. www.international-alert.org.
[14] Holder, C. D. (2004): Rainfall interception and fog precipitation in a tropical Montane cloud forest of Guatemala. – Forest Ecology and Management 190(2): 373-384. https://doi.org/doi:10.1016/j.foreco.2003.11.004. ISSN 0378-1127.
[15] Jiao, W., Chen, Y., Li, W., Zhu, C., Li, Z. (2018): Estimation of net primary productivity and its driving factors in the Ili River Valley, China. – Journal of Arid Land 10(5): 781-793. https://doi.org/10.1007/s40333-018-0022-1.
[16] Kayiranga, A., Ndayisaba, F., Nahayo, L., Karamage, F., Nsengiyumva, J., Mupenzi, C., Nyesheja, E. (2017): Analysis of climate and topography impacts on the spatial distribution of vegetation in the Virunga Volcanoes massif of east-central Africa. – Geosciences 7: 17.
[17] Kayiranga, A., Chen, B., Wang, F., Nthangeni, W., Dilawar, A., Hategekimana, Y., Zhang, H., Guo, L. (2022): Spatiotemporal Variation in Gross Primary Productivity and Their Responses to Climate in the Great Lakes Region of Sub-Saharan Africa during 2001–2020. – Sustainability (Switzerland) 14(5). https://doi.org/10.3390/su14052610.
[18] Li, J., Zou, C., Li, Q., Xu, X., Zhao, Y., Yang, W., Liu, L. (2019): Effects of urbanization on productivity of terrestrial ecological systems based on linear fitting: a case study in Jiangsu, eastern China. – Sci. Rep. 9: 17140. https://doi.org/10.1038/s41598-019-53789-9.
[19] Li, J., Zhou, K., Chen, F. (2020): Drought severity classification based on threshold level method and drought effects on NPP. – Theoretical and Applied Climatology 142(1-2): 675-686. https://doi.org/10.1007/s00704-020-03348-4.
[20] Li, H., Wu, Y., Liu, S., Xiao, J. (2021): Regional contributions to interannual variability of net primary production and climatic attributions. – Agric. For. Meteorol. 108384: 303.
[21] Li, X., Luo, Y., Wu, J. (2022): Decoupling Relationship between Urbanization and Carbon Sequestration in the Pearl River Delta from 2000 to 2020. – Remote Sensing 14(3). https://doi.org/10.3390/rs14030526.
[22] Lieth, H., Box, E. (1972): Evapotranspiration and Primary Productivity; CW Thornthwaite Memorial Model. – Publications in Climatology: The Laboratory 3(25): 37-46.
[23] Lin, H. L. (2009): A New Model of Grassland Net Primary Productivity (NPP) Based on the Integrated Orderly Classification System of Grassland. – Sixth International Conference on Fuzzy Systems and Knowledge Discovery.
[24] Liu, Y., Yang, Y., Wang, Q., Du, X., Li, J., Gang, C., Zhou, W., Wang, Z. (2019): Evaluating the responses of net primary productivity and carbon use efficiency of global grassland to climate variability along an aridity gradient. – Science of the Total Environment 652: 671-682. https://doi.org/10.1016/j.scitotenv.2018.10.295.
[25] Liu, Y., Zhou, R., Wen, Z., Khalifa, M., Zheng, C., Ren, H., Zhang, Z., Wang, Z. (2021): Assessing the impacts of drought on net primary productivity of global land biomes in different climate zones. – Ecological Indicators 130: 108146. https://doi.org/10.1016/j.ecolind.2021.108146.

[26] Ndayisaba, F., Guo, H., Bao, A., Guo, H., Karamage, F., Kayiranga, A. (2016): Understanding the spatial temporal vegetation dynamics in Rwanda. – Remote Sens. 8: 129.
[27] Nexus Profile. (2018): Nexus Country Profiles for the Niger Basin. – https://uploads.water-energy-food.org/resources/nexus_profile_niger_basin__english.pdf.
[28] Niang, I., Ruppel, O. C., Abdrabo, M. A., Essel, A., Lennard, C., Padgham, J. (2014): Africa. – In: Barros, V. R., Field, C. B., Dokken, J., Mastrandrea, M. D., Mach, K. J., Bilir, T. E., Chatterjee, M. (eds.) Climate Change 2014: Impacts, Adaptation, and Vulnerability. Part B: Regional Aspects. Contribution of Working Group II to the Fifth Assessment Report of the Intergovernmental Panel on Climate Change, pp. 1199-1265. Cambridge: Cambridge University Press.
[29] Pei, F., Li, X., Liu, X., Wang, S., He, Z. (2013): Assessing the differences in net primary productivity between pre- and post-urban land development in China. – Agricultural and Forest Meteorology 171-172: 174-186. https://doi.org/10.1016/j.agrformet.2012.12.003.
[30] Piao, S., Tan, K., Nan, H., Ciais, P., Fang, J., Wang, T., Vuichard, N. Z. B. (2012): Impacts of climate and CO_2 changes on the vegetation growth and carbon balance of Qinghai-Tibetan grasslands over the past fve decades. – Glob Planet Change 98: 73-80. https://doi.org/https://doi. org/10.1016/j.gloplacha.2012.08.009.
[31] Potter, C. S., Randerson, J. T., Field, C. B., Matson, P. A., Vitousek, P. M., Mooney, H. A., Klooster, S. A. (1993): Terrestrial ecosystem production: a process model based on global satellite and surface data. – Global Biogeochem 7: 811-841.
[32] Ren, H. Y., Wen, Z. M., Liu, Y. Y., Hu, T. M., Yang, P. H., Zhang, W., Zheng, C., Basang, C. M. (2021): Spatial-temporal Dynamics of Grassland Net Primary Productivity and its Relationship with Hydrothermic Factors in Northern China. – Acta Agrestia Sinica 29(8): 1779-1792.
[33] Rong, T., Long, L. H. (2021): Quantitative Assessment of NPP Changes in the Yellow River Source Area from 2001 to 2017. – https://doi.org/10.1088/1755-1315/687/1/012002.
[34] Sala, A. O. E., Parton, W. J., Joyce, L. A., Lauenroth, W. K. (2015): Primary Production of the Central Grassland of the United States. – JSTOR Ecology 69(1): 40-45.
[35] Sun, H., Chen, Y., Xiong, J., Ye, C., Yong, Z., Wang, Y., He, D., Xu, S. (2022): Relationships between climate change, phenology, edaphic factors, and net primary productivity across the Tibetan Plateau. – International Journal of Applied Earth Observation and Geoinformation 107: 102708. https://doi.org/10.1016/j.jag.2022.102708.
[36] Turner, D. P., Ritts, W. D., Cohen, W. B., Gower, S. T., Running, S. W., Zhao, M., Costa, M. H., Kirschbaum, A. A., Ham, J. M., Saleska, S. R., Ahl, D. E. (2006): Evaluation of MODIS NPP and GPP products across multiple biomes. – Remote Sensing of Environment 102(3-4): 282-292. https://doi.org/10.1016/j.rse.2006.02.017.
[37] UNCCD. (2007): Climate Change and Desertification. – Bonn, Germany: United Nations Convention to Combat Desertification.
[38] Wang, B., Yang, S., Lü, C., Zhang, J., Wang, Y. (2010): Comparison of net primary productivity in karst and non-karst areas : a case study in Guizhou Province, China. – Environmental Earth Sciences 59: 1337-1347. https://doi.org/10.1007/s12665-009-0121-6.
[39] Wang, H., Luo, G. P., Wang, W. S., Li, Y. M., Zheng, H. W., Hu, W. J. (2019): Retrieval of farmland soil moisture in the middle and lower reaches of the Xier River Based on Multi-source Remote Sensing Data. – Journal of Natural Resources 34: 2717-2731.
[40] Wang, Y., Xu, X., Huang, L., Yang, G., Fan, L., Wei, P., Chen, G. (2019): An improved CASA model for estimating winter wheat yield from remote sensing images. – Remote Sens. 11(9): 1088. https://doi.org/10.3390/rs11091088.
[41] Wang, C., Vera-Vélez, R., Lamb, E. G., Wu, J., Ren, F. (2022): Global pattern and associated drivers of grassland productivity sensitivity to precipitation change. – Science of the Total Environment 806. https://doi.org/10.1016/j.scitotenv.2021.151224.

http://www.aloki.hu ● ISSN 1589 1623 (Print) ● ISSN1785 0037 (Online)
DOI: http://dx.doi.org/10.15666/aeer/2106_60036022

[42] Xiang-Chao, P. (2018): Research on Ecological Civilization Construction and Environmental Sustainable Development in the New Era. – IOP Conference Series: Earth and Environmental Science 153(6). https://doi.org/10.1088/1755-1315/153/6/062080.
[43] Xuan, W., Rao, L. (2023): Spatiotemporal dynamics of net primary productivity and its influencing factors in the middle reaches of the Yellow River from 2000 to 2020. – Frontiers in Plant Science 14(January): 1-16. https://doi.org/10.3389/fpls.2023.1043807.
[44] Yin, L., Dai, E., Zheng, D., Wang, Y., Ma, L., Tong, M. (2020): What drives the vegetation dynamics in the Hengduan Mountain region, southwest China: Climate change or human activity? – Ecological Indicators 112(October 2019): 106013. https://doi.org/10.1016/j.ecolind.2019.106013.
[45] Yuan, Z., Wang, Y., Xu, J., Wu, Z. (2021): Effects of climatic factors on the net primary productivity in the source region of Yangtze River, China. – Scientific Reports 11(1): 1-11. https://doi.org/10.1038/s41598-020-80494-9.
[46] Zhang, M., Lal, R., Zhao, Y., Jiang, W., Chen, Q. (2016): Estimating net primary production of natural grassland and its spatio-temporal distribution in China. – Sci. Total Environ. 553: 184-195.
[47] Zhang, R., Liang, T., Guo, J., Xie, H., Feng, Q., Aimaiti, Y. (2018): Grassland dynamics in response to climate change and human activities in Xinjiang from 2000 to 2014. – Sci. Rep. 8: 2888. https://doi.org/10.1038/s41598-018-21089-3.
[48] Zhang, X., Xiao, W., Wang, Y., Wang, Y., Wang, H., Wang, Y., Zhu, L., Yang, R. (2020): Spatial-temporal changes in NPP and its relationship with climate factors based on sensitivity analysis in the Shiyang River Basin. – J. Earth Syst. Sci. 24: 129.
[49] Zhao, M., Running, S. W. (2010): Drought-induced reduction in global terrestrial net primary production from 2000 through 2009. – Science 329(5994): 940-943. https://doi.org/10.1126/science.1192666.
[50] Zheng, Z., Zhu, W., Zhang, Y. (2020): Direct and lagged effects of spring phenology on net primary productivity in the Alpine Grasslands on the Tibetan Plateau. – Remote Sensing 12(7): 1-14. https://doi.org/10.3390/rs12071223.
[51] Zhou, Y., Zou, S., Duan, W., Chen, Y., Takara, K., Di, Y. (2022): Analysis of energy carbon emissions from agroecosystems in Tarim River Basin, China: A pathway to achieve carbon neutrality. – Appl. Energy 325: 119842.
[52] Zhu, W. Q., Pan, Y. Z., Zhang, J. S. (2007): Estimation of net primary productivity of Chinese terrestrial vegetation based on remote sensing. – J. Plant Ecol. 31: 413-424.
[53] Zhuang, Q., He, J., Lu, Y., Ji, L., Xiao, J. L. T. (2010): Carbon dynamics of terrestrial ecosystems on the Tibetan Plateau During the 20th century: an analysis with a process-based biogeochemical model. – Glob Ecol Biogeogr 19: 649-662. https://doi.org/https://doi.org/10.111 1/j.1466-8238.2010.00559.x.

http://www.aloki.hu ● ISSN 1589 1623 (Print) ● ISSN1785 0037 (Online)
DOI: http://dx.doi.org/10.15666/aeer/2106_60036022